MATERIALS SCIENCE / МАТЕРИАЛОВЕДЕНИЕ

UDC 538.951
DOI 10.17073/0368-0797-2023-6-681-687

Original article
Оригинальная статья

Theoretical strength of austenite in the presence of a pore or vacancies in the crystal: Molecular dynamics study

I. V. Zorya[1], G. M. Poletaev[2], R. Yu. Rakitin[3]

[1] **Siberian State Industrial University** (42 Kirova Str., Novokuznetsk, Kemerovo Region – Kuzbass 654007, Russian Federation)
[2] **Polzunov Altai State Technical University** (46 Lenina Ave., Barnaul, Altai Territory 656038, Russian Federation)
[3] **Altai State University** (100 Komsomol'skii Ave., Barnaul, Altai Territory 656038, Russian Federation)

zorya.i@mail.ru

Abstract. The molecular dynamics method was used to study the influence of pores of different diameters, as well as the corresponding concentration of individual vacancies, on the theoretical strength of austenite at different temperatures. The deformation in the model was carried out by shear at a constant rate of 20 m/s. We considered a shear along two directions: [$\bar{1}\bar{1}$2] and [111]. The computational austenite cell had the shape of a rectangular parallelepiped 14.0 nm long, 14.0 nm high, and 5.1 nm wide. To describe interatomic interactions, the Lau EAM potential was used, which reproduces well the structural, energy, and elastic characteristics of austenite. The stress-strain curves obtained for both considered shear directions had a similar form. In the absence of dislocation sources, plastic deformation was carried out by the formation of dislocation dipoles (dislocations with opposite Burgers vectors). The presence of a pore significantly reduced the yield strength of austenite. In this case, it was found that single vacancies randomly scattered over the volume of the computational cell also lead to a decrease in the yield strength, but, of course, not as much as the pore. The emission of dislocations during deformation occurred by the formation of dislocation loops, as a rule, in two slip planes at once. The effect of pores and vacancies on the yield strength was stronger at low temperatures. As the temperature increased, the effect of defects on the critical stress at which dislocations were formed decreased. With an increase in the pore size, as well as the concentration of vacancies, the yield strength decreased. In this case, the strongest dependence was observed for pores up to 1 nm in diameter. The influence of the concentration of vacancies in the considered range on the yield strength turned out to be comparatively smoother and almost linear.

Keywords: molecular dynamics, austenite, dislocation, pore, vacancy, theoretical strength

For citation: Zorya I.V., Poletaev G.M., Rakitin R.Yu. Theoretical strength of austenite in the presence of a pore or vacancies in the crystal: molecular dynamics study. *Izvestiya. Ferrous Metallurgy*. 2023;66(6):681–687. https://doi.org/10.17073/0368-0797-2023-6-681-687

Теоретическая прочность аустенита при наличии в кристалле поры или вакансий: молекулярно-динамическое исследование

И. В. Зоря[1], Г. М. Полетаев[2], Р. Ю. Ракитин[3]

[1] **Сибирский государственный индустриальный университет** (Россия, 654007, Кемеровская обл. – Кузбасс, Новокузнецк, ул. Кирова, 42)
[2] **Алтайский государственный технический университет им. И.И. Ползунова** (Россия, 656038, Алтайский край, Барнаул, пр. Ленина, 46)
[3] **Алтайский государственный университет** (Россия, 656038, Алтайский край, Барнаул, Комсомольский пр., 100)

zorya.i@mail.ru

Аннотация. Методом молекулярной динамики проведено исследование влияния поры разного диаметра, а также соответствующей концентрации отдельных вакансий на теоретическую прочность аустенита при разной температуре. Деформация в модели осуществляется путем сдвига с постоянной скоростью 20 м/с. Рассматривается сдвиг вдоль двух направлений: [$\bar{1}\bar{1}$2] и [111]. Расчетная ячейка аустенита имеет форму прямоугольного параллелепипеда длиной 14,0 нм, высотой 14,0 нм и шириной 5,1 нм. Для описания межатомных взаимодействий использовался EAM потенциал Лау, хорошо воспроизводящий структурные, энергетические и упругие характеристики аустенита. Кривые напряжение – деформация, полученные для обоих рассматриваемых направлений сдвига, имеют аналогичный вид. В отсутствие источников дислокаций пластическая деформация осуществляется путем формирования дислокационных диполей

(дислокаций с противоположными векторами Бюргерса). Наличие поры существенно снижает предельную прочность аустенита. Обнаружено, что случайно разбросанные по объему расчетной ячейки одиночные вакансии также приводят к снижению предельной прочности, но, естественно, не так сильно, как пора. Испускание дислокаций порой при деформации происходит путем формирования дислокационных петель, как правило, сразу в двух плоскостях скольжения. Сильнее влияние поры и вакансий на предельную прочность наблюдается при низких температурах. При увеличении температуры влияние дефектов на критическое напряжение, при котором происходит образование дислокаций, снижается. С увеличением размера поры, как и концентрации вакансий, прочность уменьшается. При этом наиболее сильная зависимость наблюдается для пор диаметром до 1 нм. Влияние концентрации вакансий в рассматриваемом диапазоне на предельную прочность оказалось сравнительно более плавное и почти линейное.

Ключевые слова: молекулярная динамика, аустенит, дислокация, пора, вакансия, теоретическая прочность

Для цитирования: Зоря И.В., Полетаев Г.М., Ракитин Р.Ю. Теоретическая прочность аустенита при наличии в кристалле поры или вакансий: молекулярно-динамическое исследование. *Известия вузов. Черная металлургия*. 2023;66(6):681–687.
https://doi.org/10.17073/0368-0797-2023-6-681-687

Introduction

During plastic deformation, in addition to interface boundaries (such as grain boundaries and their triple junctions, interphase boundaries, and surfaces), pores and microvoids play crucial role as sources of dislocations in polycrystalline materials [1 – 3]. However, there has been relatively little research dedicated to studying the mechanisms of plastic deformation at the atomic level involving pores. To date, computer modeling has demonstrated that dislocation emission from pores during deformation is facilitated by the formation of dislocation loops [3 – 6]. The authors of [5; 6] assert that in FCC crystals, loops are formed simultaneously in two slip planes. Moreover, as the pore size increases, the critical stress required for dislocation formation decreases [5; 6].

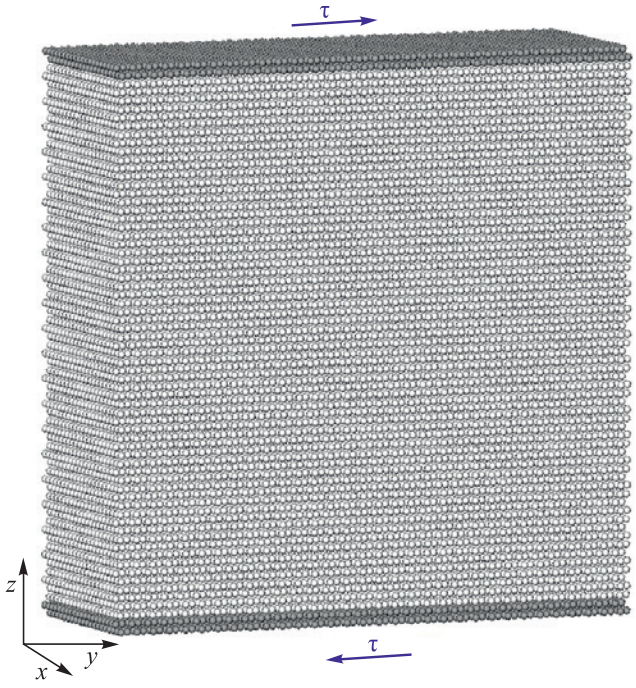

Fig. 1. Calculation cell for modeling the shift along the *y* axis (direction [$\bar{1}\bar{1}$2]) in the FCC iron

Рис. 1. Расчетная ячейка для моделирования сдвига вдоль оси *y* (направления [$\bar{1}\bar{1}$2]) в ГЦК железе

Point defects, for example, vacancies, also contribute significantly to a decrease in theoretical strength, yet the impact of their concentration on strength remains insufficiently explored, especially when compared to the effect of pore accumulations. The present study focuses on conducting a comparative analysis using molecular dynamics to investigate the influence of vacancies and pores on the theoretical strength of austenite, with consideration given to variations in temperature and vacancy concentration or pore size. Austenite garners particular interest as it serves as the foundation for many steels of considerable practical importance, such as Hadfield steel [7; 8]. Furthermore, the qualitative findings derived for austenite in this study can readily be extrapolated to other metals possessing an FCC crystal lattice.

Previously, in [9], the molecular dynamics method was employed to examine the slip velocity of edge and screw dislocations in austenite and Hadfield steel, contingent upon temperature and strain rate. The energy of formation for the aforementioned dislocations was also computed. This investigation serves as a continuation of the research documented in [9].

Model description

In the molecular dynamics model, the calculation cell representing austenite had the shape of a rectangular parallelepiped (see Fig. 1) with dimensions of 14.0 nm in length, 14.0 nm in height, and 5.1 nm in width. Initially, the cell contained 87,040 atoms. The orientation of the coordinate axes corresponded to specific crystallographic directions within the FCC lattice: *x* – [$\bar{1}$10], *y* – [$\bar{1}\bar{1}$2], *z* – [111]. The study investigated shear deformation along two directions: the *y*-axis (Fig. 1) and the *z*-axis. To induce shear in the model, atoms in the boundary regions (highlighted in dark gray in Fig. 1) were displaced. Atoms on opposite sides of the calculation cell moved in opposite directions at a constant speed of 20 m/s during the computer experiment. In previous research [9], this velocity was determined as optimal for modeling shear using the molecular dynamics method in austenite. The motion of the remaining atoms within

the computational cell was unrestricted and governed by Newton's classical equations of motion. Boundary conditions along the other axes were set as periodic.

Interatomic interactions in austenite were described using Lau's Embedded Atom Method (EAM) potential [10], known for accurately reproducing the structural, energetic, and elastic properties of austenite [10; 11]. The time integration step in the molecular dynamics method was set to 2 fs [12 – 14]. The initial velocities of atoms were assigned according to the Maxwell distribution to achieve the desired temperature. It was essential to consider the thermal expansion of the crystal lattice when setting the temperature [13 – 15]. The interatomic interaction potential employed in this study has a thermal expansion coefficient of $18 \cdot 10^{-6}$ K^{-1}, aligning well with reference data [11]. To maintain a constant temperature throughout the modeling, a Nosé–Hoover thermostat was utilized. Throughout the temperature range explored (from 100 to 1500 K), the FCC crystal lattice type remained consistent; polymorphic transformations were not considered in this investigation.

A pore was created in the center of the computational cell by removing atoms in a spherical region. The pore diameter varied from 0.6 to 2.0 nm. Vacancies were introduced by removing random atoms throughout the entire volume of the computational cell, except for the boundary layers (shown in dark gray in Fig. 1). The considered values of vacancy concentration corresponded to the number of removed atoms during the creation of pores. After the introduction of defects, a procedure of relaxation of the structure followed until an equilibrium state was achieved.

Results and discussion

Fig. 2 depicts the stress–strain dependences for the two shear orientations considered, with a constant speed of 20 m/s at a temperature of 300 K, for three scenarios: a defect-free crystal (*1*), a crystal containing 79 vacancies randomly distributed throughout its volume (*2*), and a crystal containing a pore with a diameter of 1.2 nm (*3*). The number of vacancies equaled the number of atoms removed during creation of the aforementioned pore resulting in a concentration of 0.09 % in this case.

It is widely acknowledged that the theoretical shear strength of metal crystals is exceptionally high, often exceeding 10 GPa [1; 5; 6; 16; 17]. However, introducing just one dislocation into a pristine crystal in the molecular dynamics model reduces the strength to several hundred MPa [18]. As illustrated in Fig. 2, plastic deformation in a pure austenite crystal at 300 K commenced with shear along both the *y* and *z* axes at approximately the same strain values (12.0 – 12.5 %) and stress levels (9.0 – 9.5 GPa). It is crucial to highlight that the initial ideal crystal lacked any sources of dislocation formation, including free surfaces. Consequently, the region of elastic deformation was relatively extensive.

In the absence of dislocation sources, plastic deformation occurred through the creation of dislocation dipoles, consisting of dislocations with opposite Burgers vectors. Complete dislocations promptly emerged as pairs of partial Shockley dislocations separated by a stacking fault. Typically, the distance between partial dislocations was a few nanometers, consistent with modeling findings reported by other researchers [19 – 21]. Additionally, alongside dislocation dipoles, the formation of deformation twins was also prominent during subsequent deformation stages.

As illustrated in Fig. 2, the inclusion of a pore with a diameter of 1.2 nm notably diminishes the theoretical strength: plastic shear and dislocation formation occur at significantly lower strain and stress thresholds (approxi-

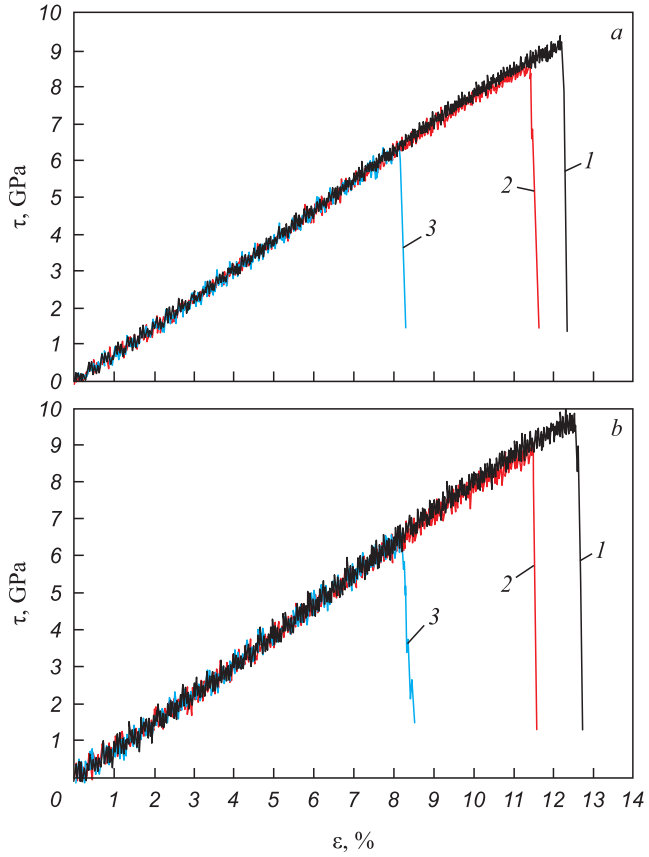

Fig. 2. Stress – strain dependences at a temperature of 300 K when shifted along the *y* axis (direction [$\bar{1}\bar{1}$2]) (*a*) and when shifted along the *z* axis (direction [111]) (*b*): *1* – in a pure FCC iron crystal; *2* – in the presence of 79 vacancies, randomly scattered over the volume of the calculation cell; *3* – in the presence of a pore with a diameter of 1.2 nm

Рис. 2. Зависимости напряжение – деформация при температуре 300 К при сдвиге вдоль оси *y* (направления [$\bar{1}\bar{1}$2]) (*a*) и при сдвиге вдоль оси *z* (направления [111]) (*b*): *1* – в чистом кристалле ГЦК железа; *2* – при наличии 79 вакансий, случайно разбросанных по объему расчетной ячейки; *3* – при наличии поры диаметром 1,2 нм

mately 8.5 % and 6 GPa, respectively). Conversely, vacancies randomly distributed throughout the computational cell, equating in number to those in the pore, exert a comparatively weaker influence on the ultimate strength. However, intriguingly, they still contribute to its reduction, with dislocations forming at a strain of about 11.5 % and a stress of 8.5 GPa. Thus, even basic point defects like vacancies attenuate the theoretical strength of the crystal.

Dislocation emission from a pore during deformation transpired via the formation of dislocation loops, aligning with findings from modeling conducted by other researchers [3 – 6]. Fig. 3 depicts examples of such loop formation from a pore with a diameter of 1.2 nm upon displacement along the *y* and *z* axes. It is evident that loops manifest in two slip planes, consistent with observations made by authors elsewhere [5; 6]. To visualize dislocations within the computational cell, an average distance to the nearest atoms visualizer was utilized, providing insight into local stretching and indirectly indicating the distribution of free volume. For each atom, the average distance to the nearest atoms was computed. If this distance deviated slightly from the distance corresponding to an ideal crystal, the atom remained uncolored; otherwise, it was assigned a color based on the deviation.

As commonly understood, temperature significantly impacts the elastic properties of materials and the likelihood of dislocation formation during deformation. Elastic moduli typically decrease nearly linearly with rising temperatures across a wide range [22 – 24], a trend often attributed to thermal expansion [22]. Plastic deformation in most materials initiates at lower stress levels as temperature increases [24 – 26].

Fig. 4 illustrates the temperature dependence of ultimate strength for shear along the *y* and *z* axes. The dependencies are presented for a defect-free crystal (*1*), a crystal containing 79 randomly scattered vacancies (*2*), and a crystal with a pore diameter of 1.2 nm (*3*). In all instances, strength diminishes with increasing temperature. Notably, as temperature rises, the influence of defects on theoretical strength diminishes. Specifically, the discrepancies in ultimate strength values between the defect-free crystal and those with vacancies or pores decrease with increasing temperature, converging toward the same value. It is pertinent to note that this convergence suggests an anticipated intersection of dependencies at the melting temperature.

Fig. 5 presents the dependencies of ultimate strength at a temperature of 300 K for shear along the *y* and *z* axes (Fig. 5, *b*) concerning the percentage of atoms c_v removed from the calculation cell in the form of individual randomly scattered vacancies or pores (designated as dependencies *1* and *2*, respectively, in Fig. 2, 4). For comparison, with a pore diameter of 1.0 nm, c_v = 0.05 %; with a pore diameter of 1.2 nm, c_v = 0.09 %; and with a pore diameter of 1.6 nm, c_v = 0.23 %.

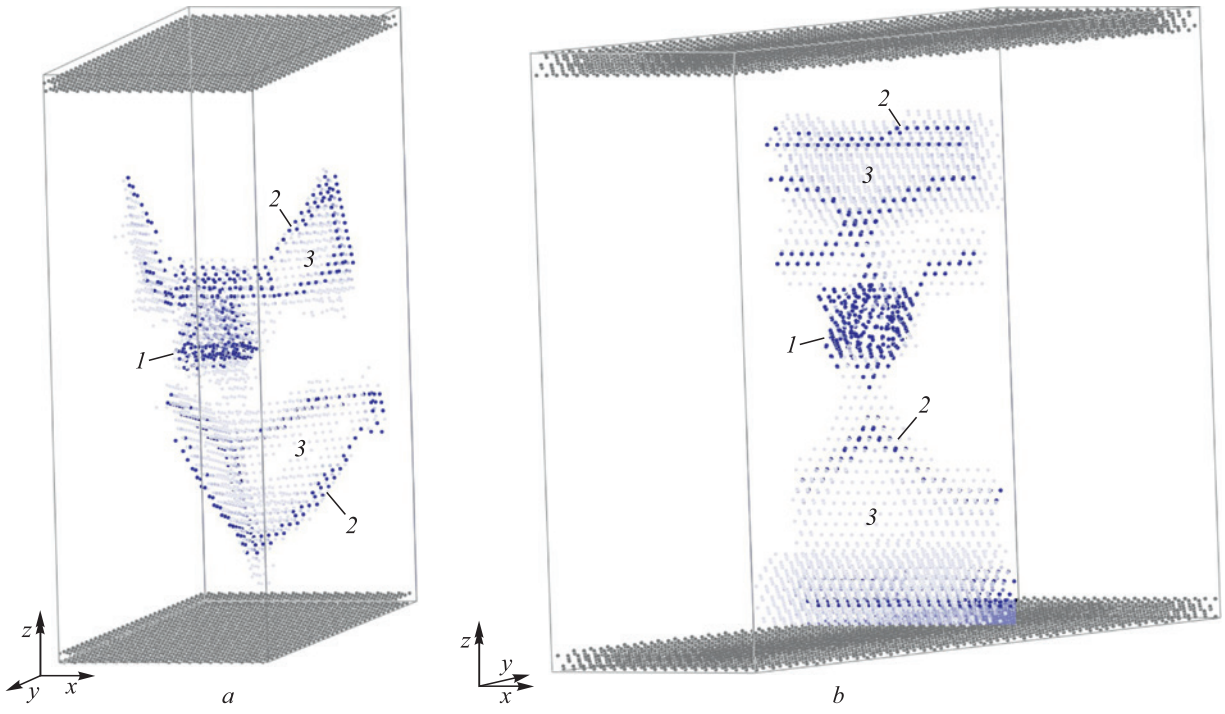

Fig. 3. Emission of dislocations by a pore in the form of dislocation loops when shifted along the *y* axis (*a*) and when shifted along the *z* axis (*b*):
1 – pore; *2* – partial dislocation; *3* – packaging defect

Рис. 3. Испускание дислокаций порой в виде дислокационных петель при сдвиге вдоль оси *y* (*a*) и оси *z* (*b*):
1 – пора; *2* – частичная дислокация; *3* – дефект упаковки

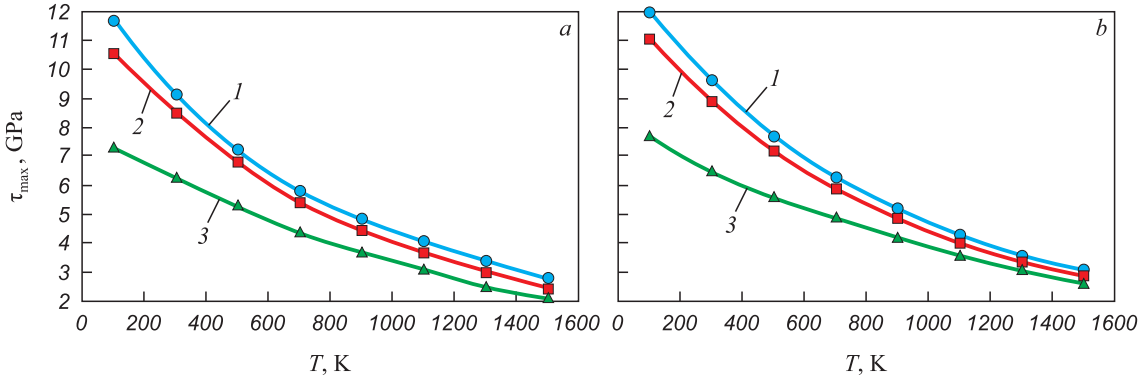

Fig. 4. Dependences of strength on temperature when shifted along the *y* axis (direction [$\bar{1}\bar{1}$2]) (*a*) and when shifted along the *z* axis (direction [111]) (*b*):
1 – in a pure FCC iron crystal; *2* – in the presence of 79 vacancies randomly scattered over the volume calculation cell; *3* – in the presence of a pore with a diameter of 1.2 nm

Рис. 4. Зависимости прочности от температуры при сдвиге вдоль оси *y* (направления [$\bar{1}\bar{1}$2]) (*a*) и при сдвиге вдоль оси *z* (направления [111]) (*b*):
1 – в чистом кристалле ГЦК железа; *2* – при наличии 79 вакансий, случайно разбросанных по объему расчетной ячейки; *3* – при наличии поры диаметром 1,2 нм

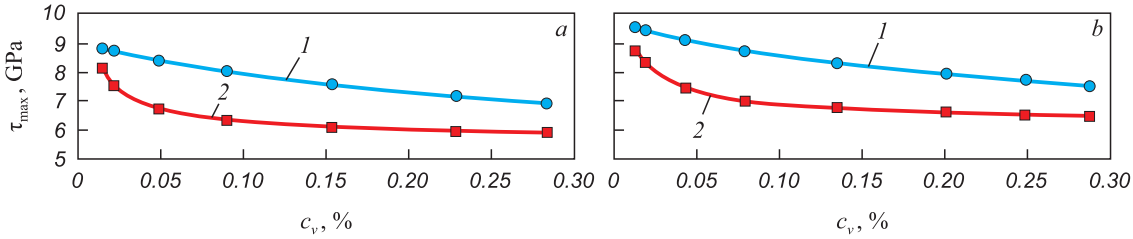

Fig. 5. Dependences of strength at temperature of 300 K on the number of atoms removed from the calculated cell in the form of randomly scattered vacancies (*1*) or pores (*2*) when shifted along the *y* axis (directions [$\bar{1}\bar{1}$2]) (*a*) and when shifted along the *z* axis (directions [111]) (*b*)

Рис. 5. Зависимости прочности при температуре 300 К от количества удаленных из расчетной ячейки атомов в виде случайно разбросанных вакансий (*1*) или поры (*2*) при сдвиге вдоль оси *y* (направления [$\bar{1}\bar{1}$2]) (*a*) и при сдвиге вдоль оси *z* (направления [111]) (*b*)

As evident, an increase in both vacancy concentration and pore radius correlates with a reduction in strength. Notably, the most pronounced dependence is observed for small pore sizes, up to approximately 1 nm. Beyond this range, while strength continues to decrease with increasing pore radius, the rate of decline is notably less pronounced compared to smaller pore sizes. Conversely, the influence of vacancy concentration within the considered range on theoretical strength is more gradual and nearly linear.

Conclusions

The influence of pores of varying diameters, along with the corresponding concentration of individual vacancies, on the theoretical strength of austenite across different temperatures was investigated using the molecular dynamics method. Deformation in the model was induced by shearing at a constant speed of 20 m/s, considering shifts along two directions: [$\bar{1}\bar{1}$2] and [111]. Stress-strain dependences obtained for both shear directions exhibited similar trends. In the absence of dislocation sources, plastic deformation ensued through the formation of dislocation dipoles characterized by dislocations with opposite Burgers vectors. The presence of pores substantially reduced the ultimate strength of austenite, while single vacancies randomly dispersed throughout the computational cell also contributed to a decrease in ultimate strength, albeit to a lesser extent compared to pores. Dislocation emission from pores during deformation occurred through the formation of dislocation loops, typically manifesting in two slip planes simultaneously. A more pronounced impact of pores and vacancies on ultimate strength was observed at lower temperatures. However, as temperature increased, the influence of defects on the critical stress at which dislocation formation occurred diminished. Moreover, with increasing pore size and vacancy concentration, the strength exhibited a decreasing trend. Notably, the strongest dependence was observed for pores with diameters up to 1 nm. The effect of vacancy concentration within the considered range on ultimate strength was relatively smoother and displayed an almost linear behavior.

References / Список литературы

1. Seppälä E.T., Belak J., Rudd R.E. Three-dimensional molecular dynamics simulations of void coalescence during dynamic fracture of ductile metals. *Physical Review B*. 2005;71(6):064112. https://doi.org/10.1103/PhysRevB.71.064112
2. Bobylev S.V., Morozov N.F., Ovid'ko I.A. Dislocation emission by pores in nanocrystalline metals. *Physics of the Solid State*. 2007;49(6):1098–1103. https://doi.org/10.1134/S1063783407060133
3. Ruestes C.J., Bringa E.M., Stukowski A., Rodríguez Nieva J.F., Tang Y., Meyers M.A. Plastic deformation of a porous bcc metal containing nanometer sized voids. *Computational Materials Science*. 2014;88:92–102. http://dx.doi.org/10.1016/j.commatsci.2014.02.047
4. Wang Y., Bi W., Deng L., Zhang X., Tang J., Wang L. Study on the relationship between surface and dislocation of nanoporous copper under cyclic shear loading. *AIP Advances*. 2022;12(3):035318. https://doi.org/10.1063/5.0085569
5. Traiviratana S., Bringa E.M., Benson D.J., Meyers M.A. Void growth in metals: Atomistic calculations. *Acta Materialia*. 2008;56(15):3874–3886. https://doi.org/10.1016/j.actamat.2008.03.047
6. Bringa E.M., Traiviratana S., Meyers M.A. Void initiation in fcc metals: Effect of loading orientation and nanocrystalline effects. *Acta Materialia*. 2010;58(13):4458–4477. https://doi.org/10.1016/j.actamat.2010.04.043
7. Zhang F.C., Lv B., Wang T.S., Zheng C.L., Zhang M., Luo H.H., Liu H., Xu A.Y. Explosion hardening of Hadfield steel crossing. *Materials Science and Technology*. 2010; 26(2):223–229. https://doi.org/10.1179/174328408X363263
8. Chen C., Lv B., Ma H., Sun D., Zhang F. Wear behavior and the corresponding work hardening characteristics of Hadfield steel. *Tribology International*. 2018;121:389–399. https://doi.org/10.1016/j.triboint.2018.01.044
9. Zorya I.V., Poletaev G.M., Rakitin R.Yu. Energy and velocity of sliding of edge and screw dislocations in austenite and Hadfield steel: Molecular dynamics simulation. *Izvestiya. Ferrous Metallurgy*. 2022;65(12):861–868. (In Russ.). https://doi.org/10.17073/0368-0797-2022-12-861-868

   Зоря И.В., Полетаев Г.М., Ракитин Р.Ю. Энергия и скорость скольжения краевой и винтовой дислокаций в аустените и стали Гадфильда: молекулярно-динамическое моделирование. *Известия вузов. Черная металлургия*. 2022;65(12):861–868. https://doi.org/10.17073/0368-0797-2022-12-861-868
10. Lau T.T., Forst C.J., Lin X., Gale J.D., Yip S., Van Vliet K.J. Many-body potential for point defect clusters in Fe-C alloys. *Physical Review Letters*. 2007;98(21):215501. https://doi.org/10.1103/PhysRevLett.98.215501
11. Oila A., Bull S.J. Atomistic simulation of Fe-C austenite. *Computational Materials Science*. 2009;45(2):235–239. https://doi.org/10.1016/j.commatsci.2008.09.013
12. Chen C., Zhang F., Xu H., Yang Z., Poletaev G.M. Molecular dynamics simulations of dislocation–coherent twin boundary interaction in face-centered cubic metals. *Journal of Materials Science*. 2022;57:1833–1849. https://doi.org/10.1007/s10853-021-06837-7
13. Poletaev G.M. Self-diffusion in liquid and solid alloys of the Ti–Al system: Molecular-dynamics simulation. *Journal of Experimental and Theoretical Physics*. 2021;133(4): 455–460. https://doi.org/10.1134/S1063776121090041
14. Poletaev G.M., Novoselova D.V., Kaygorodova V.M. The causes of formation of the triple junctions of grain boundaries containing excess free volume in fcc metals at crystallization. *Solid State Phenomena*. 2016;247:3–8. https://doi.org/10.4028/www.scientific.net/SSP.247.3
15. Poletaev G.M., Zorya I.V. Influence of light impurities on the crystal-melt interface velocity in Ni and Ag. Molecular dynamics simulation. *Technical Physics Letters*. 2020;46(6): 575–578. https://doi.org/10.1134/S1063785020060231
16. Bukreeva K.A., Iskandarov A.M., Dmitriev S.V., Umeno Y., Mulyukov R.R. Theoretical shear strength of FCC and HCP metals. *Physics of the Solid State*. 2014;56(3):423–428. https://doi.org/10.1134/S1063783414030081
17. Li P.-T, Yang Y.-Q., Xia Zh., Luo X., Jin N., Gao Y., Liu G. Molecular dynamic simulation of nanocrystal formation and tensile deformation of TiAl alloy. *RSC Advances*. 2017;7:48315–48323. https://doi.org/10.1039/C7RA10010H
18. Krasnikov V.S., Kuksin A.Yu., Mayer A.E., Yanilkin A.V. Plastic deformation under high-rate loading: the multiscale approach. *Physics of the Solid State*. 2010;52(7):1386–1396. https://doi.org/10.1134/S1063783410070115
19. Zhao Sh., Osetsky Yu.N., Zhang Y. Atomic-scale dynamics of edge dislocations in Ni and concentrated solid solution NiFe alloys. *Journal of Alloys and Compounds*. 2017;701: 1003–1008. https://doi.org/10.1016/j.jallcom.2017.01.165
20. Rodney D., Ventelon L., Clouet E., Pizzagalli L., Willaime F. Ab initio modeling of dislocation core properties in metals and semiconductors. *Acta Materialia*. 2017;124:633–659. https://doi.org/10.1016/j.actamat.2016.09.049
21. Hunter A., Beyerlein I.J., Germann T.C., Koslowski M. Influence of the stacking fault energy surface on partial dislocations in fcc metals with a three-dimensional phase field dislocations dynamics model. *Physical Review B*. 2011;84(14):144108. https://doi.org/10.1103/PhysRevB.84.144108
22. Shtremel' M.A. *Strength of Alloys. Part 1. Lattice Defects*. Moscow: Metallurgiya; 1982:280. (In Russ.).

    Штремель М.А. *Прочность сплавов. Ч. 1. Дефекты решетки*. Москва: Металлургия; 1982:280.
23. Киттель Ч. *Введение в физику твердого тела*. Москва: Наука, 1978:792.

    Kittel Ch. *Elementary Solid State Physics*. John Wiley & Sons; 1962:339.
24. Guo J., Wen B., Melnik R., Yao Sh., Li T. Molecular dynamics study on diamond nanowires mechanical properties: Strain rate, temperature and size dependent effects. *Diamond and Related Materials*. 2011;20(4):551–555. https://doi.org/10.1016/j.diamond.2011.02.016
25. Tachibana T., Furuya H., Koizumi M. Dependence on strain rate and temperature shown by yield stress of uranium dioxide. *Journal of Nuclear Science and Technology*. 1976;13(9):497–502. https://doi.org/10.1080/18811248.1976.9734063
26. Cereceda D., Diehl M., Roters F., Raabe D., Perlado J.M., Marian J. Unraveling the temperature dependence of the yield strength in single-crystal tungsten using atomistically-informed crystal plasticity calculations. *International Journal of Plasticity*. 2016;78:242–265. https://doi.org/10.1016/j.ijplas.2015.09.002

Information about the Authors / Сведения об авторах

Irina V. Zorya, *Dr. Sci. (Phys.-Math.), Assist. Prof., Head of the Chair of Heat-Gas-Water Supply, Water Disposal and Ventilation,* Siberian State Industrial University
ORCID: 0000-0001-5748-813X
E-mail: zorya.i@mail.ru

Gennadii M. Poletaev, *Dr. Sci. (Phys.-Math.), Prof., Head of the Chair of Advanced Mathematics,* Polzunov Altai State Technical University
ORCID: 0000-0002-5252-2455
E-mail: gmpoletaev@mail.ru

Roman Yu. Rakitin, *Cand. Sci. (Phys.-Math.), Assist. Prof., Director of College,* Altai State University
ORCID: 0000-0002-6341-2761
E-mail: movehell@gmail.ru

Ирина Васильевна Зоря, *д.ф.-м.н., доцент, заведующий кафедрой теплогазоводоснабжения, водоотведения и вентиляции,* Сибирский государственный индустриальный университет
ORCID: 0000-0001-5748-813X
E-mail: zorya.i@mail.ru

Геннадий Михайлович Полетаев, *д.ф.-м.н., профессор, заведующий кафедрой высшей математики,* Алтайский государственный технический университет им. И.И. Ползунова
ORCID: 0000-0002-5252-2455
E-mail: gmpoletaev@mail.ru

Роман Юрьевич Ракитин, *к.ф.-м.н., доцент, директор колледжа,* Алтайский государственный университет
ORCID: 0000-0002-6341-2761
E-mail: movehell@gmail.ru

Contribution of the Authors / Вклад авторов

I. V. Zorya – problem statement, analysis of literary sources, processing of results, writing the main text.
G. M. Poletaev – problem statement, development of a computer model, analysis of literary sources, processing of results, editing the final version of the article.
R. Yu. Rakitin – creating a computer model, performing calculations, obtaining results, obtaining drawings and graphs.

И. В. Зоря – постановка задачи, анализ литературных источников, обработка результатов, написание основного текста статьи.
Г. М. Полетаев – постановка задачи, разработка компьютерной модели, анализ литературных источников, обработка результатов, редактирование финальной версии статьи.
Р. Ю. Ракитин – создание компьютерной модели, проведение расчетов и получение результатов, получение рисунков и графиков для статьи.

Received 06.02.2023
Revised 27.02.2023
Accepted 20.07.2023

Поступила в редакцию 06.02.2023
После доработки 27.02.2023
Принята к публикации 20.07.2023